Global Journal of Researches in Engineering: E
Civil And Structural Engineering
Volume 16 Issue 4 Version 1.0 Year 2016
Type: Double Blind Peer Reviewed International Research Journal
Publisher: Global Journals Inc. (USA)
Online ISSN: 2249-4596 & Print ISSN: 0975-5861

Effect of Some Factors on the Dynamic Response of Reinforced Cylindrical Shell with a Hole on Elastic Supports Subjected to Blast Loading

By Nguyen Thai Chung & Le Xuan Thuy
Le Quy Don Technical University

Abstract- This paper presents the finite element algorithm and calculation method of reinforced cylindrical shell with a hole under blast loading. Using the programmed algorithm and computer program written in Matlab environment, the authors solved a specific problem, from which examining the effects of structural and loading parameters to the dynamic response of the shell.

Keywords: *cylindrical shell reinforced, blast loading, hole.*

GJRE-E Classification: *FOR Code: 090599*

Strictly as per the compliance and regulations of :

© 2016. Nguyen Thai Chung & Le Xuan Thuy. This is a research/review paper, distributed under the terms of the Creative Commons Attribution-Noncommercial 3.0 Unported License http://creativecommons.org/licenses/by-nc/3.0/), permitting all non commercial use, distribution, and reproduction in any medium, provided the original work is properly cited.

Effect of Some Factors on the Dynamic Response of Reinforced Cylindrical Shell with a Hole on Elastic Supports Subjected to Blast Loading

Nguyen Thai Chung [α] & Le Xuan Thuy [σ]

Abstract- **This paper presents the finite element algorithm and calculation method of reinforced cylindrical shell with a hole under blast loading. Using the programmed algorithm and computer program written in Matlab environment, the authors solved a specific problem, from which examining the effects of structural and loading parameters to the dynamic response of the shell.**

Keywords: cylindrical shell reinforced, blast loading, hole.

I. Introduction

Dao Huy Bich and Vu Do Long [1] used the analytical method to analyze the dynamics response of imperfect functionally graded material shallow shells subjected to dynamic loads. Nivin Philip, C. Prabha [2] analyzed static buckling of the stiffened composite cylindrical shell subjected to external pressure by the finite element method. Nguyen Thai Chung and Le Xuan Thuy [3] used the finite element method to analyze the dynamic of eccentrically rib-stiffened shallow cylindrical shells on flexible couplings under blast loadings. Lin Jing, Zhihua Wang, Longmao Zhao [4], Gabriele Imbalzano, Phuong Tran, Tuan D. Ngo, Peter V.S. Lee [5], Phuong Tran, Tuan D. Ngo, Abdallah Ghazlan [6] analyzed dynamic response of the composite shells and cylindrical sandwich shells under blast loading. Yonghui Wang, Ximei Zhai, Siew Chin Lee, Wei Wang [7] succeeded in analyzing the dynamic responses of curved steel-concrete-steel sandwich shells subjected to blast loading by the numerical method. Anqi Chen, Luke A. Louca and Ahmed Y. Elghazouli [8] analyzed dynamic behaviour of cylindrical steel drums under blast loading conditions. However, studies on the calculation of shell structure under the effect of the shock waves are few, especially of the shells with a hole.

In order to develop the study approach to the shallow cylindrical shells, in this paper, the authors set the algorithm and computer program to analyze the dynamics of rib-stiffened shallow cylindrical shells with abatement holes under the effect of the shock wave loads. Couplings on the shell borders are elastic supports with the tension- compression stiffness k.

II. Computational Model and Assumptions

Considering the eccentrically rib-stiffened shallow cylindrical shell on elastic supports, being described by springs with stiffness k. The shell is subjected to a layer shock wave. Because the shell is shallow, the shock-wave presssure affecting can be considered to be uniformly distributed over the surface of the shell (Figure 1).

The assumptions: Materials of the shell are homogeneous and isotropic; the rib and shell are linearly elastically deformed and have absolutely adhesive connection; loading process works, no cracks appearing around the hole.

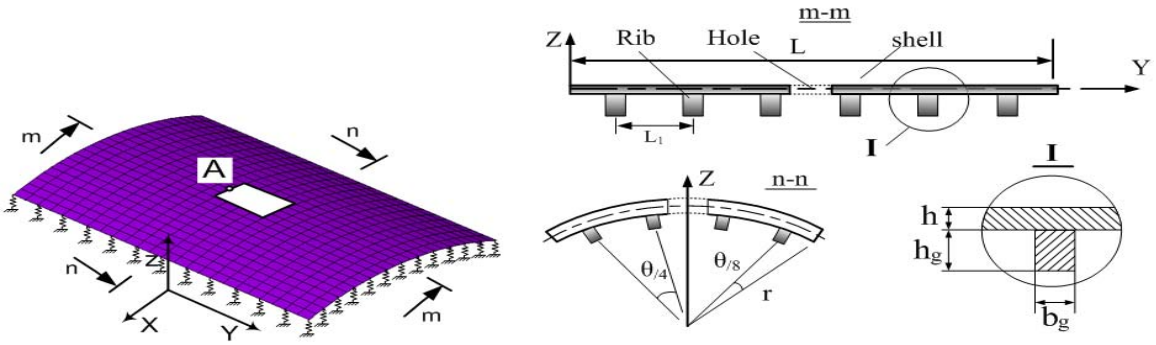

Figure 1: Problem model

Author α σ: Department of Solid Mechanics, Le Quy Don Technical University, Ha Noi, Viet Nam. e-mails: thaichung1273@gmail.com, thuylxmta@gmail.com

© 2016 Global Journals Inc. (US)

III. Finite element Model and basic Equations

a) Types of elements to be used

The shell is fragmented by 4-node flat shell elements, which means that the shell is a finite combination of 4-node flat elements, is a combination of membrane elements and plate elements subject to bending and twisting combination (Figure 2).

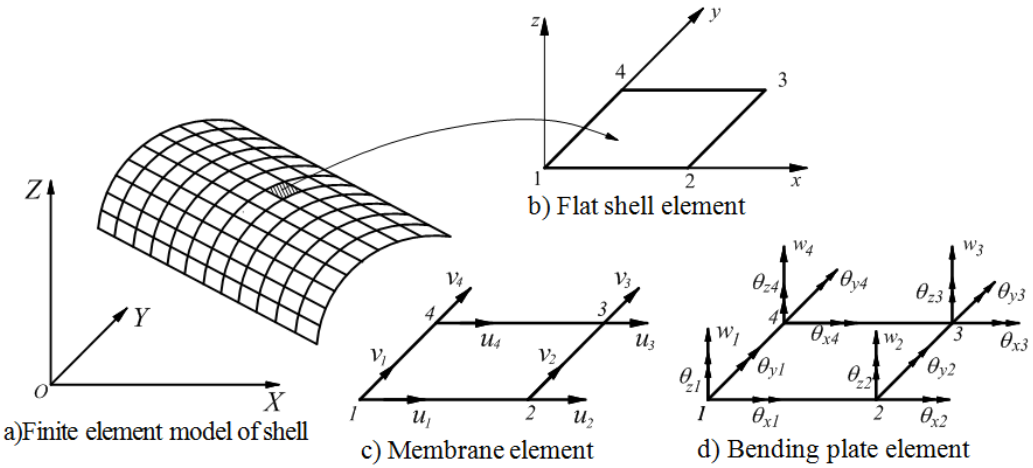

Figure 2: General shell element model

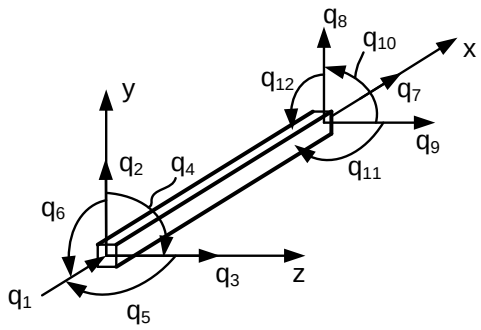

Figure 3: Beam elements

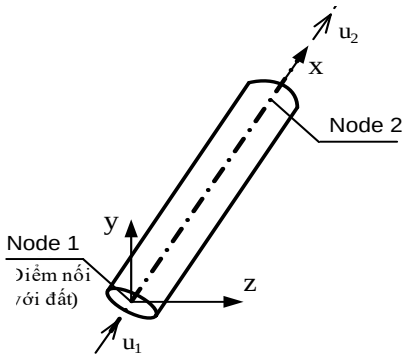

Figure 4: Bar elements

The stiffened ribs are divided into 2-node spatial beam elements, each node has 6 degrees of freedom (Figure 3). The linearly elastic supports are described by bar elements, that are under tension and compression along its axis denoted by *x*, each node of the element has one degree of freedom (Figure 4) [9],[10].

b) Flat shell element describes the shell

Each node of the shell element is composed of 6 degrees of freedom: u_i, v_i, w_i, θ_{xi}, θ_{yi}, θ_{zi}. Displacement of any point of the element can be written as [9]:

$$\begin{aligned} u(x,y,z,t) &= u_0(x,y,t) + z\theta_y(x,y,t), \\ v(x,y,z,t) &= v_0(x,y,t) - z\theta_x(x,y,t), \\ w(x,y,z,t) &= w_0(x,y,t), \\ \theta_x = \theta_x(x,y,t),\ \theta_y &= \theta_y(x,y,t),\ \theta_z = \theta_z(x,y,t) \end{aligned} \quad (1)$$

where u, v, and w are the displacements along x, y and z axes, respectively; superscript "o" denotes mid plane displacement; and θ_x, θ_y, and θ_z are rotations about the x - axis, y - axis and z - axis, respectively. Strain vector components are:

$$\varepsilon_x = \frac{\partial u}{\partial x},\ \varepsilon_y = \frac{\partial v}{\partial y},\ \gamma_{xy} = \frac{\partial u}{\partial y} + \frac{\partial v}{\partial x}, \quad (2)$$

Relationship stress - strain can be written as

$$\{\sigma\} = [D]\{\varepsilon\}, \quad (3)$$

where [D] is a matrix of relationship stress - strain.

Using Hamilton's principle for the elements [12]:

$$\delta H_e = \delta \int_{t_0}^{t_1} (T_e - U_e + W_e)\,dt = 0, \quad (4)$$

where $H_e = T_e - U_e + W_e = H_e\left(\{q^e\},\{\dot{q}^e\},t\right)$ is the Hamilton function, T_e is the kinetic energy of the element, U_e is the total potential energy of the element, W_e is total external

© 2016 Global Journals Inc. (US)

work due to mechanical loading of element e, $\{q^e\},\{\dot{q}^e\}$ are vector of nodal displacements, and vector of nodal velocities, respectively.

Considering the case not mention the damping, from (4) leads to the following:

$$-\frac{d}{dt}\left\{\frac{\partial H_e}{\partial\{\dot{q}^e\}}\right\}+\frac{\partial H_e}{\partial\{q^e\}}=\{0\}, \quad (5)$$

The kinetic energy T_e of the elements is determined by the expression [9]:

$$T_e=\frac{1}{2}\{\dot{q}^e\}^T\left(\int_{V_e}\rho[N]^T[N]dV_e\right)\{\dot{q}^e\} =\frac{1}{2}\{\dot{q}^e\}^T[M]_e^s\{\dot{q}^e\}, \quad (6)$$

where [N] is function matrix of flat shell elements [9], [10], V_e is element volume, $[M]_e^s$ is element mass matrix, ρ is specific volume of materials.

The total potential energy U_e is determined by:

$$U_e=\frac{1}{2}\{q^e\}^T[K]_e^s\{q^e\}, \quad (7)$$

In which $[K]_e^s$ is stiffness matrix of flat shell elements.

Total external work due to mechanical loading is determined by:

$$W_e=\frac{1}{2}\int_{V_e}\{q^e\}^T\{f_b^e\}dV_e+ +\frac{1}{2}\int_{S_e}\{q^e\}^T\{f_s^e\}d\ _e\{+Aq^e\}^T\{f_c^e\}, \quad (8)$$

with A_e is element area, $\{f_b^e\}$-volume force vector, $\{f_s^e\}$-surface force vector, $\{f_c^e\}$- concentrated force vector of the elements [9], [10].

Substitute (6), (7), (8) into (4), (5), we have the differential equation describing the vibration of the shell element in matrix form as follow:

$$[M]_e^s\{\ddot{q}^e\}+[K]_e^s\{q^e\}=\{F^e\}, \quad (9)$$

where $\{q^e\}$ is the vector of nodal displacements, $\{F^e\}$ is the mechanical force vector.

In the (X, Y, Z) coordinate system:

$$[M']_e^s=[T]_e^T[M]_e^s[T], \quad [K']_e^s=[T]_e^T[K]_e^s[T] \quad (10)$$

$[T]_e$ is the coordinate axes transition matrix [9].

b) Space Beam Element Describes the Rib

Displacement in any node of the bar with (x, y) coordinates is identified as follows [9]:

$$u=u(x,y,z,t)=u_0(x,t)+z\theta_y(x,t)-y\theta_z(x,t)$$
$$v=v(x,y,z,t)=v_0(x,y,t)-z\theta_x(x,t), \quad (11)$$
$$w(x,y,z,t)=w_0(x,t)+y\theta_z(x,t)$$

where, the subscript "0" represents axis x (y = 0, z = 0), t represents time; u, v and w are the displacements along x, y and z; θ_x is the rotation of cross section about the longitudinal axis x; and θ_y and θ_z denote rotations of the cross section about y and z axes.

The strain components:

$$\varepsilon_x=\frac{\partial u}{\partial x}=\frac{\partial u_0}{\partial x}+z\frac{\partial\theta_y}{\partial x}-y\frac{\partial\theta_z}{\partial x},$$
$$\gamma_{zx}=\frac{\partial u}{\partial z}+\frac{\partial w}{\partial x}=\frac{\partial w_0}{\partial x}+y\frac{\partial\theta_x}{\partial x}+\theta_y, \quad (12)$$
$$\gamma_{xy}=\frac{\partial u}{\partial y}+\frac{\partial v}{\partial x}=\frac{\partial v_0}{\partial x}-z\frac{\partial\theta_x}{\partial x}-\theta_z.$$

Node displacement vector: $\{q\}_e^b=\{q_1, q_2, q_3, q_4, q_5, q_6, q_7, q_8, q_9, q_{10}, q_{11}, q_{12}\}^T$ (13)

Element stiffness matrix is set up from 4 types of component stiffness matrices [9], [11]:

$$\underbrace{[K]_e^b}_{12x12}=\underbrace{[K_x]_e}_{2x2}+\underbrace{[K_r]_e}_{2x2}+\underbrace{[K_{xy}]_e}_{4x4}+\underbrace{[K_{xz}]_e}_{4x4} \quad (14)$$

where, $[K_x]_e=(k_x^{ij})$, $[K_r]_e=(k_r^{ij})$, i, j = 1,2; $[K_{xy}]_e=(k_{xy}^{lk})$, $[K_{xz}]_e=(k_{xz}^{lk})$, l, k = 1÷4, are tension (compression) stiffness matrix, torsion stiffness matrix, bending stiffness matrix in the xy plane, and bending stiffness matrix in the xz plane, respectively.

© 2016 Global Journals Inc. (US)

$$[K]_e^b = \begin{bmatrix}
k_x^{11} & 0 & 0 & 0 & 0 & 0 & k_x^{12} & 0 & 0 & 0 & 0 & 0 \\
0 & k_{xy}^{11} & 0 & 0 & 0 & k_{xy}^{12} & 0 & k_{xy}^{13} & 0 & 0 & 0 & k_{xy}^{14} \\
0 & 0 & k_{xz}^{11} & 0 & k_{xz}^{12} & 0 & 0 & 0 & k_{xz}^{13} & 0 & k_{xz}^{14} & 0 \\
0 & 0 & 0 & k_r^{11} & 0 & 0 & 0 & 0 & 0 & k_r^{12} & 0 & 0 \\
0 & 0 & k_{xz}^{21} & 0 & k_{xz}^{22} & 0 & 0 & 0 & k_{xz}^{23} & 0 & k_{xz}^{24} & 0 \\
0 & k_{xy}^{21} & 0 & 0 & 0 & k_{xy}^{22} & 0 & k_{xy}^{23} & 0 & 0 & 0 & k_{xy}^{24} \\
k_x^{21} & 0 & 0 & 0 & 0 & 0 & k_x^{22} & 0 & 0 & 0 & 0 & 0 \\
0 & k_{xy}^{31} & 0 & 0 & 0 & k_{xy}^{32} & 0 & k_{xy}^{33} & 0 & 0 & 0 & k_{xy}^{34} \\
0 & 0 & k_{xz}^{31} & 0 & k_{xz}^{32} & 0 & 0 & 0 & k_{xz}^{33} & 0 & k_{xz}^{34} & 0 \\
0 & 0 & 0 & k_r^{21} & 0 & 0 & 0 & 0 & 0 & k_r^{22} & 0 & 0 \\
0 & 0 & k_{xz}^{41} & 0 & k_{xz}^{42} & 0 & 0 & 0 & k_{xz}^{43} & 0 & k_{xz}^{44} & 0 \\
0 & k_{xy}^{41} & 0 & 0 & 0 & k_{xy}^{42} & 0 & k_{xy}^{43} & 0 & 0 & 0 & k_{xy}^{44}
\end{bmatrix} \tag{15}$$

Similarly, element mass matrix is also established from 4 types of volume matrix:

$$\underbrace{[M]_e^b}_{12x12} = \underbrace{[M_x]_e}_{2x2} + \underbrace{[M_r]_e}_{2x2} + \underbrace{[M_{xy}]_e}_{4x4} + \underbrace{[M_{xz}]_e}_{4x4} \tag{16}$$

$$[M]_e^b = \begin{bmatrix}
m_x^{11} & 0 & 0 & 0 & 0 & 0 & m_x^{12} & 0 & 0 & 0 & 0 & 0 \\
0 & m_{xy}^{11} & 0 & 0 & 0 & m_{xy}^{12} & 0 & m_{xy}^{13} & 0 & 0 & 0 & m_{xy}^{14} \\
0 & 0 & m_{xz}^{11} & 0 & m_{xz}^{12} & 0 & 0 & 0 & m_{xz}^{13} & 0 & m_{xz}^{14} & 0 \\
0 & 0 & 0 & m_r^{11} & 0 & 0 & 0 & 0 & 0 & m_r^{12} & 0 & 0 \\
0 & 0 & m_{xz}^{21} & 0 & m_{xz}^{22} & 0 & 0 & 0 & m_{xz}^{23} & 0 & m_{xz}^{24} & 0 \\
0 & m_{xy}^{21} & 0 & 0 & 0 & m_{xy}^{22} & 0 & m_{xy}^{23} & 0 & 0 & 0 & m_{xy}^{24} \\
m_x^{21} & 0 & 0 & 0 & 0 & 0 & m_x^{22} & 0 & 0 & 0 & 0 & 0 \\
0 & m_{xy}^{31} & 0 & 0 & 0 & m_{xy}^{32} & 0 & m_{xy}^{33} & 0 & 0 & 0 & m_{xy}^{34} \\
0 & 0 & m_{xz}^{31} & 0 & m_{xz}^{32} & 0 & 0 & 0 & m_{xz}^{33} & 0 & m_{xz}^{34} & 0 \\
0 & 0 & 0 & m_r^{21} & 0 & 0 & 0 & 0 & 0 & m_r^{22} & 0 & 0 \\
0 & 0 & m_{xz}^{41} & 0 & m_{xz}^{42} & 0 & 0 & 0 & m_{xz}^{43} & 0 & m_{xz}^{44} & 0 \\
0 & m_{xy}^{41} & 0 & 0 & 0 & m_{xy}^{42} & 0 & m_{xy}^{43} & 0 & 0 & 0 & m_{xy}^{44}
\end{bmatrix} \tag{17}$$

In the (X, Y, Z) coordinate system:

$$[K']_e^s = [T]_e^T [K]_e^b [T], \quad [M']_e^b = [T]_e^T [M]_e^b [T].$$

c) Bar Element Describes the Elastic support

Node displacement vector and stiffness matrix of bar element is [9]:

$$\{q\}_e^{sp} = \{u_1, u_2\}^T, \quad \underbrace{[K]_e^{sp}}_{2\times2} = k_{sp}\begin{bmatrix} 1 & -1 \\ -1 & 1 \end{bmatrix} \tag{18}$$

where, k_{sp} is the tension- compression stiffness of elastic support.

d) Governing equations and solving method

The connection of bar elements and space beam elements into the flat shell elements forming the rib-stiffened shell – elastic support system is implemented by direct stiffness method and Skyline diagram under the general algorithm of Finite element method [9],[10]. After connecting and getting rid of margins, the governing equations of the rib-stiffened shell – elastic support system is:

$$[M]\{\ddot{q}\} + [K]\{q\} = \{F\}, \tag{19}$$

© 2016 Global Journals Inc. (US)

In the case of taking the damping into account the equation (19) becomes:

$$[M]\{\ddot{q}\}+[C]\{\dot{q}\}+[K]\{q\}=\{F\}, \qquad (20)$$

where:

$[M]=\sum_e [M]_e^s+\sum_e [M]_e^b$ - overall mass matrix (after getting rid of margins);

$$[K]=\sum_e [K]_e^s+\sum_e [K]_e^b+\sum_e [K]_e^{sp}$$

- overall stiffness matrix (after getting rid of margins).

$[C]=\alpha[M]+\beta[K]$ - overall damping matrix, α, β are Rayleigh damping coefficients [10].

Equation (20) is a linear dynamic equation and may be solved by using the Newmark's direct integration method. Based on the established algorithm the authors have written the program called Stiffened_SC_Shell_Withhole in Matlab environment.

IV. Numerical Examination

a) The effects of abatement hole

Considering the shallow cylindrical shell whose plan view is a rectangular, generating line's length *l* = 3.0m, opening angle of the shell $\theta = 40^o$, the radius of curvature is r = 2.0m, shell thickness th = 0,02m. The shell material has elastic modulus $E = 2.2\times10^{11}$ N/m^2, Poisson coefficient $\nu = 0.31$, specific volume $\rho = 7800$kg/m^3. The eccentrically ribbed shell with the height of ribs $h_g = 0.03$m, thickness of ribs $th_g = 0.006$m, the shell with 4 ribs is parallel to the generating line, 6 ribs is perpendicular to the generating line, the ribs are equispaced. The ribs' material has $E = 2.4\times10^{11}$N/m^2, $\nu = 0.3$, $\rho = 7000$kg/m^3. Considering the problem with two cases:

- Case 1 (*basic problem*): The shell has a square (a x a) abatement hole in the middle position, with a = 0.3 m;

- Case 2: The shell has no hole (a = 0).

Acting load: the shock waves act uniformly to the direction of normal on the shell surface according to the law: $p(t)=p_{max}F(t)$, $F(t)=\begin{cases}1-\frac{t}{\tau}: & 0\le t\le\tau\\ 0: & t>\tau\end{cases}$, p_{max} = 3.10^4 N/m^2, $\tau = 0.05$s.

Conditions of coupling: Four sides of the shells with couplings are limited to move horizontally and leaned on elastic supports with the tension- compression stiffness k = $3.5\text{x}10^4$ kN/m.

Case 1: The shell has a square abatement hole with the side a = 0.3 m (Basic problem):

Using the established Stiffened_SC_Shell _ with hole program, the authors solved the problem with the calculating time t_{cal} = 0.08s, integral time step Δt = 0.0005s. The results of deflection response and stress at the midpoint of the hole edge (*point A*) are shown in Figures 5, 6.

Case 2: The shell has no hole:

Results in Figures 7 and 8 respectively are deflection response and stress at the midpoint of the shell.

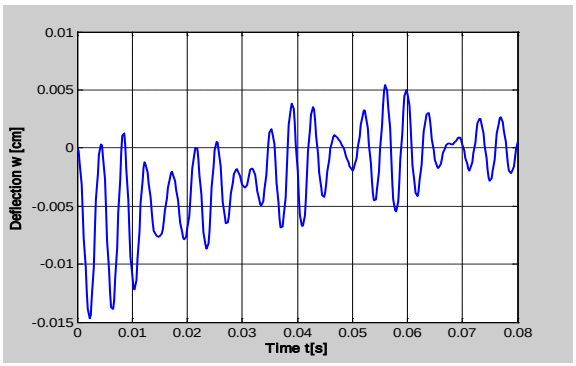

Figure 5: Displacement response w at point A

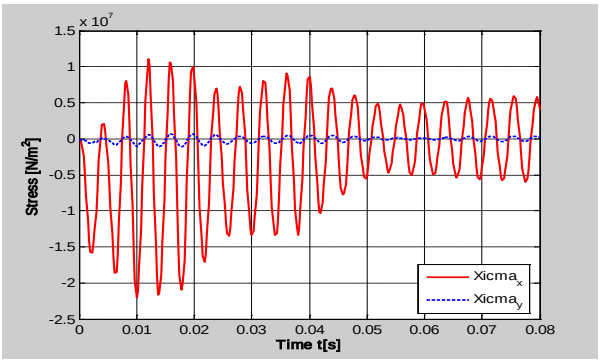

Figure 6: Stress response σ_x, σ_y at point A

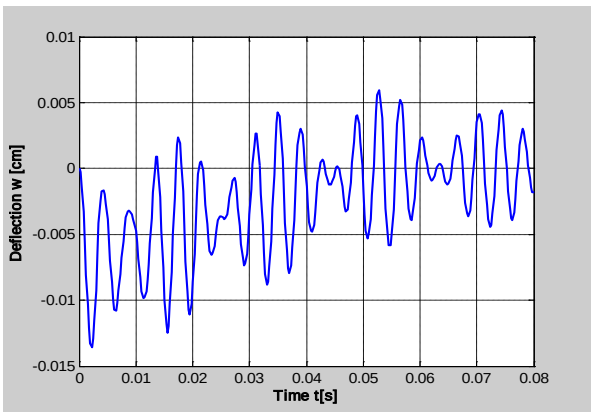

Figure 7: Displacement response wat the midpoint of the shell

© 2016 Global Journals Inc. (US)

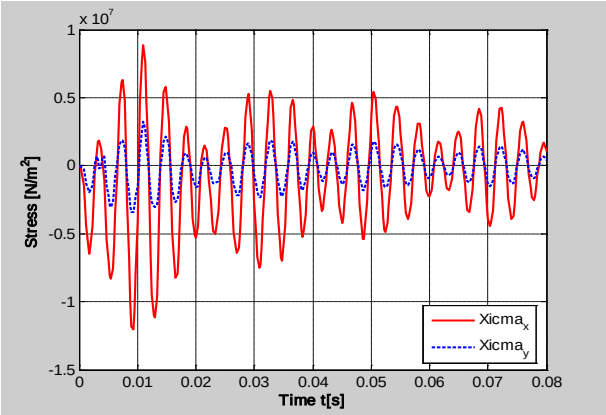

Figure 8: Stress response σ_x, σ_y at the midpoint of the shell

Table 1: Comparison of the values of displacements and stresses in two cases

	Deflection W_z^{max} [cm]	Stress σ_x^{max} [N/m^2]	Stress σ_y^{max} [N/m^2]
Case 1	0.01471	$21.964.10^6$	$1.111.10^6$
Case 2	0.01358	$12.009.10^6$	$3.423.10^6$

Comment: When there is a hole, both displacements and stresses in the structure are increased. Especially, the maximum stress in the structure increases rapidly. This explains the destruction vulnerability of the structure when it has defects.

b) The effects of the size of the hole

Examining the problem with the size of the hole changes: a_1 = 0.15 m, a_2 = 0.25 m, a_3 = 0.30 m. Displacement response and real-time stresses at point A corresponding to cases shown in Figures 9, 10.

Table 2: Extreme values of calculated quantities at point A when the size a changes

a [m]	W_z^{max} [cm]	Stress σ_x^{max} [N/m^2]	Stress σ_y^{max} [N/m^2]
0.15	0.01577	$20.389.10^6$	$1.212.10^6$
0.25	0.01521	$20.716.10^6$	$1.808.10^6$
0.30	0.01471	$21.964.10^6$	$1.111.10^6$

Comment: Generally, when increasing the size of the abatement hole, point A shifts closer to the stiffening rib, so the stiffness of the area surrounding point A increases, making the displacement of point A reduces, stress increases.

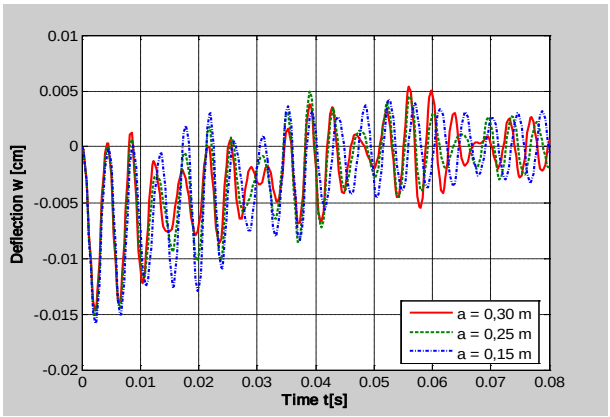

Figure 9: Deflection response w at point A based on a

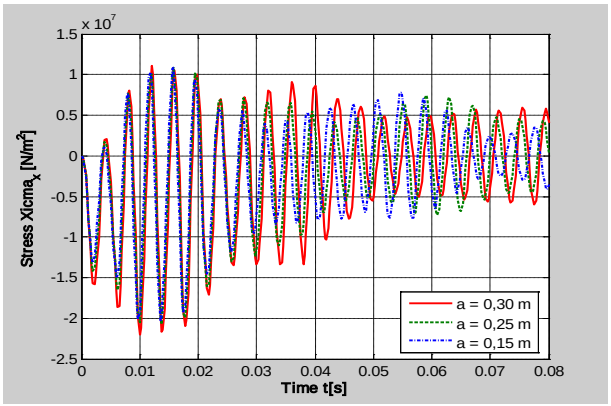

Figure 10: Stress response σ_x at point A based on a

c) The effects of radius r

Examining the problem with r changes: r_1 = 2.0 m, r_2 = 2.3 m, r_3 = 2.5 m, r_4 = 2.8 m, r_5 = 3.0 m. Extreme values of the deflection and stresses at the calculated point are expressed in table 3 and Figures 11 ÷ 14.

© 2016 Global Journals Inc. (US)

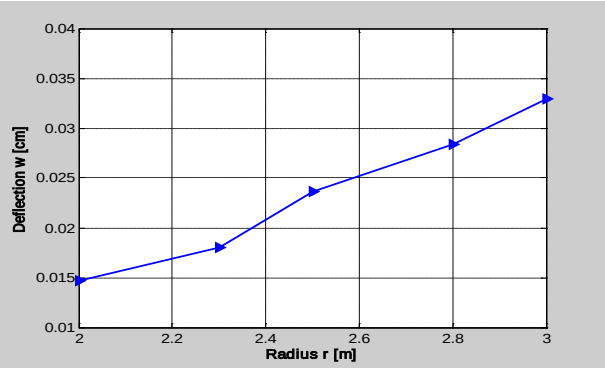

Figure 11: Deflection response w when changing r

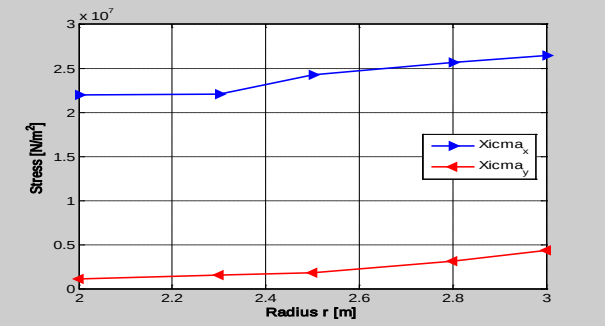

Figure 12: Stress response σ_x, σ_y when changing r

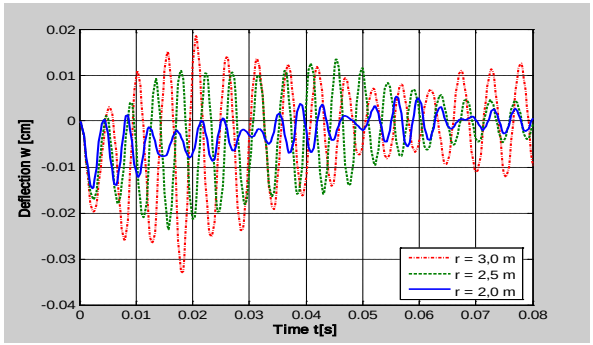

Figure 13: Deflection response w with various values of r

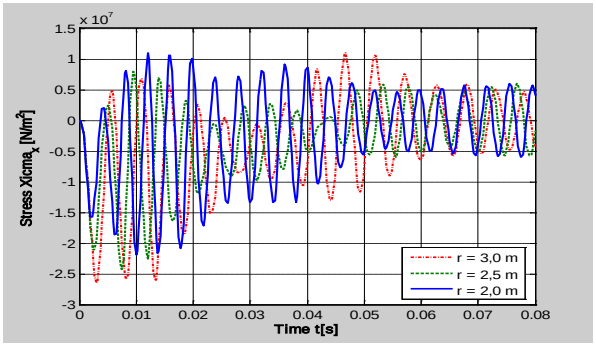

Figure 14: Stress response σ_x with various values of r

Comment: When preserving the opening angle of the shell and other parameters, increasing the radius r will increase the displacement and stress at the calculated point. At this time, the vibration of the structure increases rapidly (Figure 13).

Table 3: Extreme values of calculated quantities at point A when the size r changes

r [m]	W_z^{max} [cm]	Stress σ_x^{max} [N/m^2]	Stress σ_y^{max} [N/m^2]
2.0	0.01471	$21.964.10^6$	$1.111.10^6$
2.3	0.01799	$22.556.10^6$	$1.499.10^6$
2.5	0.02361	$24.284.10^6$	$1.841.10^6$
2.8	0.02837	$25.654.10^6$	$3.140.10^6$
3.0	0.03298	$26.448.10^6$	$4.340.10^6$

d) The effects of the height of rib

Assessing the effects of the height of the stiffening rib, the authors examined the problem with h_g changes: h_{g1} = 0.03 m, h_{g2} = 0.04 m, h_{g3} = 0.05 m, h_{g4} = 0.06 m, h_{g5} = 0.07 m. Displacement response and real-time stresses at point A corresponding to cases shown in Figures 15, 16, 17, 18.

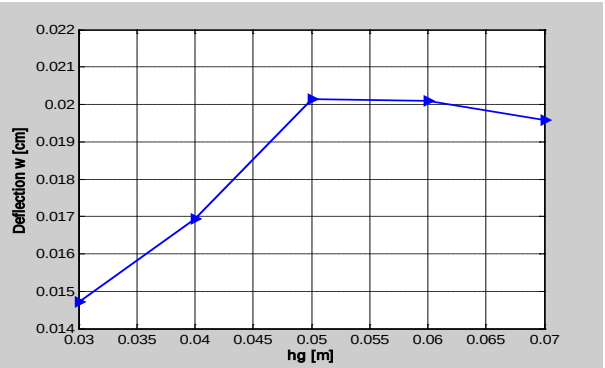

Figure 15: Deflection response w when changing h_g

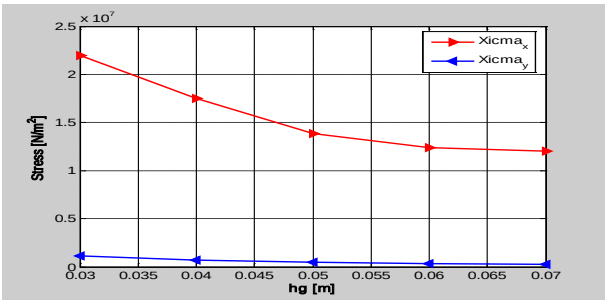

Figure 16: Stress response σ_x, σ_y when changing h_g

© 2016 Global Journals Inc. (US)

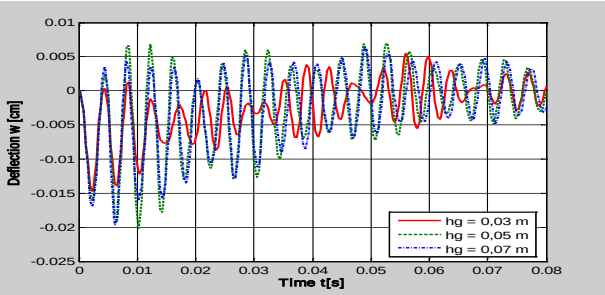

Figure 17: Deflection response w with various values of h_g

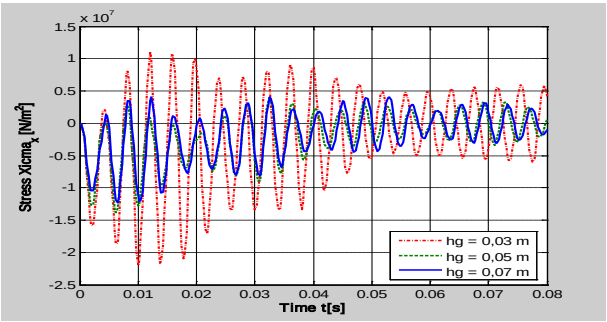

Figure 18: Stress response σ_x with various values of h_g

Comment: In the examined value range of h_g, while increasing h_g, stresses σ_x, σ_y at the calculated point reduce nonlinearly. The displacement at the initial calculated point increases (h_g = 0.03m ÷ 0.05 m), then decreases (h_g = 0.06m ÷ 0.07 m). This can be explained as follow: When increasing the height of rib, the stiffness of the shell increases making it less deformed. However, the shell uses the elastic seat connection, so when the stiffness of the shell increases making more load transfers to the elastic seating which leads to the increase of the total displacement of the calculated point. In phase h_g = 0.06m ÷ 0.07m, after the seating shifts down fully to become a hard seating, this time, the stabler stiffness structure will make the shell less deformed, so the displacement at the calculated point reduces compared to the previous case (h_g = 0.05m).

Table 4: Extreme values of calculated quantities at point A when changing the size of h_g

h_g [m]	W_z^{max} [cm]	Stress σ_x^{max} [N/m^2]	Stress σ_y^{max} [N/m^2]
0.03	0.01471	$21.964.10^6$	$1.111.10^6$
0.04	0.01694	$17.487.10^6$	$0.706.10^6$
0.05	0.02014	$13.857.10^6$	$0.477.10^6$
0.06	0.02010	$12.361.10^6$	$0.340.10^6$
0.07	0.01958	$12.052.10^6$	$0.272.10^6$

V. Conclusions

The paper had:

– Set up the governing equations of system, finite element algorithm and computer program to analyze the dynamics of the rib-stiffened shallow shells with a holes on elastic supports under the effect of the blast loading.

– Examined some structural factors such as: hole size, curve radius, height of rib, thereby making the assessment of the influence level of these factors to the dynamic response of the mentioned shell.

The results of the paper can be used as a reference for the calculation and design of similar structures, with any hole.

References Références Referencias

1. Dao Huy Bich, Vu Do Long (2010), Nonlinear dynamic analysis of imperfect functionally graded material shallow shells, *Vietnam Journal of Mechanics, VAST, Vol.32, No.1 (2010), pp.1-14.*
2. Nivin Philip, C.Prabha (2013), Numerical investigation of stiffened composite cylindrical shell subjected to external pressure, *International Journal of Emerging technology and Advanced Engineering, volume 3, issue 3, March 2013, pp.591-598.*
3. Nguyen Thai Chung, Le Xuan Thuy (2015), Analysis of the Dynamics of Eccentrically Rib-stiffened shallow cylindrical shells on Flexible Couplings under the effect of the blast loadings, *Journal of Construction, No. 4.2015, Viet Nam, pp.73-76.*
4. Lin Jing, Zhihua Wang, Longmao Zhao (2013), Dynamic response of cylindrical sandwich shells with metallic foam cores under blast loading – Numerical simulations, *Composite Structures 99 (2013), pp.213-223.*
5. Gabriele Imbalzano, Phuong Tran, Tuan D. Ngo, Peter V.S. Lee (2016), A numerical study of auxetic composite panels under blast loadings, *Composite Structures 135(2016), pp.339-352.*
6. Phuong Tran, Tuan D. Ngo, Abdallah Ghazlan (2016), Numerical modelling of hybrid elastomeric composite panels subjected to blast loadings, *Composite Structures 153(2016), pp.108-122.*
7. Yonghui Wang, Ximei Zhai, Siew Chin Lee, Wei Wang (2016), Responses of curved steel-concrete-steel sandwich shells subjected to blast loading, *Thin-Walled Structures 108(2016), pp.185-192.*
8. Anqi Chen, Luke A. Louca, Ahmed Y. Elghazouli (2016), Behaviour of cylindrical steel drums under blast loading conditions, *International Journal of Impact Engineering 88(2016), pp.39-53.*
9. O. C. Zienkiewicz, Taylor R. L. (1998), *The Finite Element Method*, McGraw-Hill, International Edition.
10. Young W.Kwon, Hyochoong Bang (1997), *The finite element method using Matlab*, CRC mechanical engineering series.
11. Nguyen Thai Chung, Hoang Hai, Shin Sang Hee (2016), Dynamic Analysis of High Building with Cracks in Column Subjected to Earthquake

© 2016 Global Journals Inc. (US)

Loading, *American Journal of Civil Engineering, 2016; 4(5), pp.233-240.*
12. (2006), Advanced Dynamics of Structures, NTUST - CT 6006.

© 2016 Global Journals Inc. (US)